Thermal Characterization of Planar Transformer – Merits of a Novel Extended-Core Geometry

Mangesh Borage, Sunil Tiwari and Swarna Kotaiah
Power Supplies Division
Centre for Advanced Technology
Indore 452 013, India
e-mail: mbb@cat.ernet.in

***Abstract*—Superior thermal performance due to high surface area to volume ratio is a principal advantage of planar transformers. The low-profile flat nature provides a large surface area for cooling the core and removal of heat from the windings. However it is observed in the experimental studies that in planar transformers, a considerable portion of the windings protrudes out from both sides of the core resulting in ineffective heat removal and radiated EMI from the winding portion outside the core. Novel extended-core geometry proposed in this paper, in which the ferrite core is extended to cover the exposed winding portion, alleviates aforementioned problems. Preliminary results of the finite-element analysis demonstrate the effectiveness of proposed structure in shielding. To characterize the effectiveness of heat removal from the windings a thermal model is defined considering average temperature rise of core and windings. A step by step experimental procedure is explained to derive the parameters of the model. Comparative thermal characterization of conventional and extended-core geometry of planar transformers is performed. It is shown that the proposed structure enhances the heat removal from the windings thereby reducing its temperature rise.**

I. INTRODUCTION

Ever increasing switching frequency is continuously shrinking the size of power converter circuits mainly due to reduction in the size of magnetic and filter components. The size of magnetic components (transformer and inductors) however does not proportionally decrease since the design of high frequency magnetic components is loss-limited. Planar transformers are meritoriously used now a days to enhance the power density due to following principal advantages [1]-[5]: Excellent predictability and repeatability due to pre-tooled components, low leakage inductance, minimum skin effect and better thermal management due to high ratio of core surface area to volume.

In non-planar magnetics, power loss in the windings is transferred partially to ambient and mostly on the central limb of the core. Since the distance of this core center point from core surface is significant, a large temperature gradient exists. A hot spot is thus created in non-planar structures, which is not accessible directly for heat removal. This forces the designer to use lower current densities for the windings to keep resistive losses within limit. In planar magnetic components, power loss in the windings is transferred (due to the planar winding structure) not to the central limb of core but to the upper and bottom limbs, which are thin, wide and in close contact with the heat sink. Thus the power loss in the windings can be extracted easily allowing a designer to use higher current density for the windings.

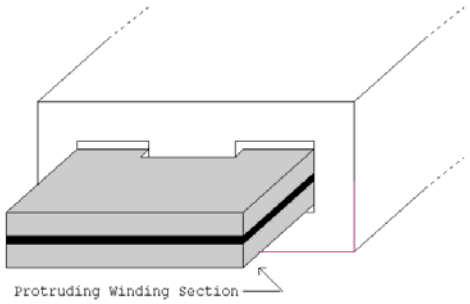

Fig.1: Schematic diagram of a section of planar transformer showing the exposed winding sections protruding outside the core.

In planar transformers, a considerable portion of the windings protrudes out from both sides of the core (see figure 1). It is observed in the experimental work presented in this paper that the heat removal from the winding portion outside the core is not effective. Furthermore, the uncovered windings result in radiated EMI. Novel extended core geometry for the planar transformers is presented which alleviates aforementioned problems. The extended core geometry is realized by extending the upper and lower limbs of the planar E-I structure to cover the winding portion protruding outside. These sections do not contribute to the normal functioning of transformer, but enhance heat removal and shield the winding to reduce radiated EMI.

The major objectives of the paper are: (1) To characterize the effectiveness of heat removal from the windings and to define a thermal model considering average temperature rise of core and windings. (2) To develop a step by step experimental procedure to derive the parameters of the model. (3) To validate the correctness of model with independent experiments. (4) To perform comparative thermal characterization of conventional and extended-core geometry of planar transformers. (5) To qualitatively demonstrate the effective-

ness of proposed structure in shielding using finite-element simulation results.

II. Prototype Planar Transformer

A prototype planar transformer is developed for use in a 1 kW (20V/50A) power supply using two-switch forward converter operating at 100 kHz. The design parameters of the transformer are given in table 1. The standard multi-layer etched PCBs were not used in this prototype development due to high currents. Instead, planar windings were made by pasting copper foils on a 5 mil mylar sheet and developing required winding pattern on them. Primary uses a copper foil of 0.1 mm thickness and for secondary copper foil of 0.2 mm thickness was used. The choice of copper thickness was dictated by availability and moreover, the winding thickness was not optimized for minimum loss in this prototype fabrication. Primary is a spiral winding structure with three turns per layers, each turn being 3 mm wide. Secondary is single turn per layer, each 10 mm wide. Resulting current densities are 18.6 A/mm^2 for primary and 14 A/mm^2 for secondary. Fig. 2 shows the winding patterns for primary and secondary. A photograph of prototype planar transformer during assembly is shown in Fig. 3. It is clearly seen that a significant portion of the winding remains outside the core. This protruding portion of the winding poses following potential problems:

TABLE 1

MAJOR PARAMETERS OF PROTOTYPE PLANAR TRANSFORMER

Turns ratio	6:1
Core	2* ELP 43/10/28 with I 43/4/28
N_p	18
N_s	3
Peak flux density	0.2 T
$I_{s(rms)}$	33.5 A
$I_{p(rms)}$	5.6 A

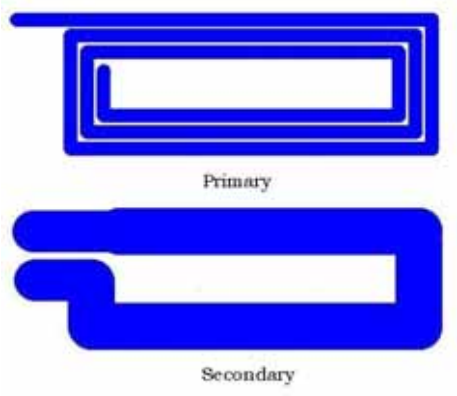

Fig.2: Winding patterns of the prototype planar transformer.

Fig.3: Photograph of conventional prototype planar transformer clearly showing that the large section of the windings protrude outside the core from both sides of the transformer.

(1) The heat removal of the winding portion inside the core is through core to the heat sink. However, the portion outside the core hangs in free air and heat removal depends on natural convection, which may not be effective in high density converters. Therefore, the temperature of winding portion outside the core is higher than the portion covered by core. During preliminary tests the local temperature of the winding outside the core is observed to be higher than the average temperature of the windings. (The average temperature of the winding and method of its measurement is described subsequently.)
(2) High frequency currents passing through the windings give rise to EMI through this uncovered portion of coil. In modern-day high-density converters, wherein the transformer and power circuit and control electronics in incorporated on a single printed circuit board, the radiated EMI can adversely affect the functioning of the circuit.

III. Novel Extended-Core Geometry

The problems encountered due to winding portion protruding outside the core can be alleviated if the transformer core could be extended to cover the exposed winding. Novel extended-core geometry for the planar transformers presented in this paper follows this principle. The extended core geometry is realized by extending the upper and lower limbs of the planar E-I structure to cover the winding portion protruding outside. These sections do not contribute to the normal functioning of transformer, but enhance heat removal and shield the windings. Such a structure can easily be realized by placing I-sections (Fig. 4a) of planar E-I pairs directly above and beneath the windings. The extended core can also be of planar U-U form as shown in Fig. 4b.

A photograph of prototype extended-core planar transformer is shown in Fig. 5. The design parameters of this prototype are the same as those listed in table 1. The winding design, copper and insulation thickness is the same as those for the conventional prototype planar transformer. In the prototype development the extended-core geometry uses I-section of the planar core.

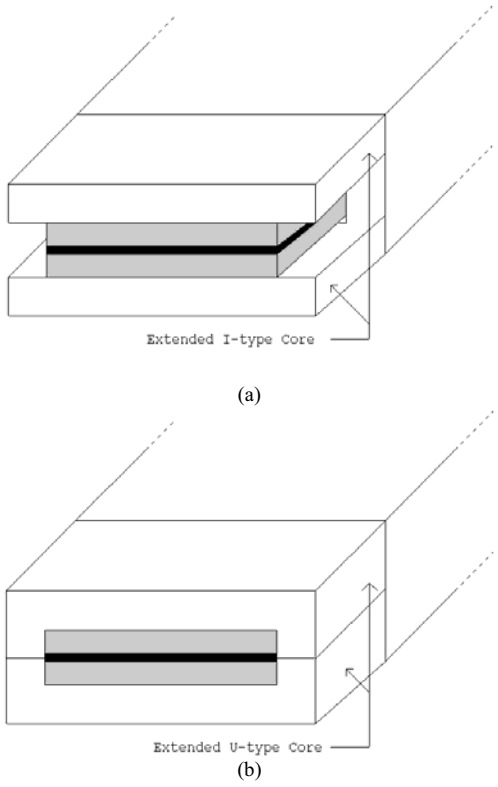

Fig.4: Schematic diagram of a section of proposed extended-core planar transformer using (a) I-type core, and, (b) U-type core.

Fig.5: Photograph of prototype extended-core planar transformer.

Heat removal from core (due to winding and core loss) is assisted by mounting and clamping the core on a heat sink for both – conventional and extended-core prototype planar transformers. An aluminium clamp is in close thermal contact with the heat sink over the entire length of the transformer. Therefore, it can be assumed that the core and the heatsink are approximately at the same temperature and the temperature gradient is negligible. Figure 6 shows the assembled extended-core planar transformer with heatsink and aluminium clamps.

In the subsequent sections, the experimental thermal characterization of the prototypes and results of finite element studies are described to ascertain the merits of proposed extended-core geometry.

IV. Thermal Characterization of Planar Transformers

A. Measurement of Average Temperature Rise of winding

Planar windings being very compact, it is difficult to measure temperature rise of the winding by placing or inserting temperature sensor. All layers of a winding are not at the same temperature and there is temperature gradient between layers. The gradient, however, is small in planar structures due to aforementioned reasons and it is sufficient to measure the average temperature rise of the winding. If we pass current I through a winding of n layers temperature of each layer of winding will change by ΔT_1, ΔT_2, ΔT_3,…. ΔT_n. Electrical resistance of copper changes with temperature depending on its temperature coefficient of resistance (α). Using this material property, we can measure the average change in temperature of the winding as described below.

Let R_{cold} be the resistance of each winding layer at ambient temperature. Terminal voltage across the winding at ambient temperature,

$$V_{cold} = nIR_{cold} \tag{1}$$

Temperature of winding increases due to the power loss. Electrical resistance of the winding of i^{th} layer of winding is given by,

$$R_{hot,i} = R_{cold}\left(1 + \alpha\Delta T_i\right) \tag{2}$$

Terminal voltage across winding in the "hot" condition is,

$$V_{hot} = V_{cold} + \alpha IR_{cold}\sum_{i=1}^{n}\Delta T_i \tag{3}$$

Thus, average temperature rise of the winding is given by,

$$\frac{\sum_{i=1}^{n}\Delta T_i}{n} = \left(\frac{V_{hot} - V_{cold}}{V_{cold}}\right)\frac{1}{\alpha} \tag{4}$$

Fig.6: Photograph of completed prototype extended-core planar transformer with heatsink and clamp

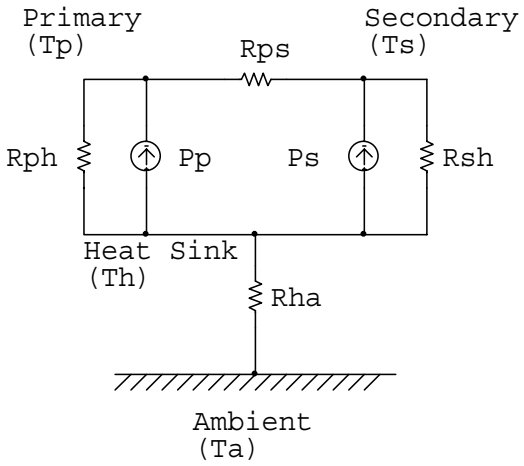

Fig.7: Thermal model of the planar transformer.

B. Measurement of Average Temperature Rise of Heatsink

The mounting and clamping of transformer cores on heatsink and the symmetrical heat transfer from core to heat sink avoids large temperature gradients along the heat sink. Average temperature rise of heat sink can then be measured by placing multiple sensors selectively at different location and then averaging their values. In the present measurement, we place LM 335 temperature sensor (with 10 mV/^{o}C sensitivity) at three locations.

C. Thermal Model

Using the analogy of thermal and electrical systems, the thermal model to characterize the heat transfer from windings can be drawn as shown in figure 7 considering average temperature rise of core and windings. The losses are represented by current sources and the thermal resistances are represented by electrical resistances. Various symbols are defined as under:

P_p = Copper loss in primary winding
P_s = Copper loss in secondary winding
R_{ph}= Thermal resistance between primary and heat sink
R_{sh}= Thermal resistance between secondary and heat sink
R_{ps}= Thermal resistance between primary and secondary
R_{ha} =Thermal resistance of heat sink to ambient
T_p = Average temperature of primary winding
T_s = Average temperature of secondary winding
T_h = Average temperature of heat sink
T_a = Ambient temperature

Following simple tests help to derive the model parameters.

1. Resistance of primary and secondary windings at ambient temperature: The resistances can be determined accurately by passing low, constant current through primary winding and measuring the terminal voltage.

2. Temperature rise of primary winding due to losses in primary: The average temperature rise of primary winding due to losses in itself can be measured by passing full-load equivalent dc current through the winding and monitoring the rise in the terminal voltage. Secondary winding is left open. Sufficient time (approximately 30 minutes) is allowed for the steady-state to reach before noting the readings. Under this condition, it can be derived from the thermal model of Fig. 7 that,

$$T_p - T_h = \frac{R_{ph}\left(R_{ps} + R_{sh}\right)}{R_{ph} + R_{sh} + R_{ps}} P_p \tag{5}$$

3. Temperature rise of secondary winding due to losses in secondary: Similar to previous test-2, the temperature rise of secondary due to losses in itself can be measured by passing dc current through the secondary and leaving primary winding open. It can be shown that, under this condition,

$$T_s - T_h = \frac{R_{sh}\left(R_{ps} + R_{ph}\right)}{R_{ph} + R_{sh} + R_{ps}} P_s \tag{6}$$

4. Temperature rise of primary winding due to losses in secondary: While performing previous test-3, a small dc current is passed through primary winding and terminal voltage of primary winding is measured. From fig. 7,

$$\frac{T_s - T_h}{T_p - T_h} = \frac{\left(R_{ps} + R_{ph}\right)}{R_{ph}} \tag{7}$$

The data obtained from tests 1through 4 can easily be used to solve eqn. (5) through (7) and determine R_{ps}, R_{ph} and R_{sh}. Since temperature rise of heat sink is also monitored during the tests, we can also determine R_{ha}.

D. Test Set-up

The discussion in previous section suggests that a number of tests are required to be carried out for the thermal characterization of planar transformer. Figure 8 shows schematically the test set-up established for this purpose. Two current-controlled dc power supplies are used to pass required constant dc current in the primary and secondary windings. Two sets of voltage taps monitor the terminal voltage of the windings. The average temperature rise of the heatsink is monitored by mounting three LM 335 temperature sensors along the surface of the transformer and averaging their readings. The voltage taps from the winding terminals and the leads of temperature sensors are connected to the multi-channel data acquisition system, the latter being interfaced with a personal computer for data logging. The data is collected in the computer and is then processed with spreadsheet software to calculate various parameters.

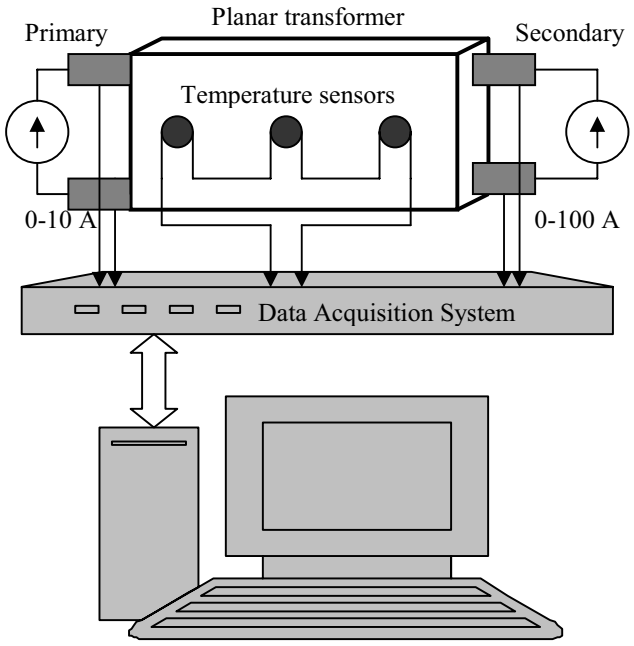

Fig.8: Experimental test set-up for thermal characterization of planar transformers.

V. Experimental Results

The tests described in previous section are performed on the conventional and proposed planar transformer prototypes. To minimize measurement errors, multiple set of data is recorded and the results are averaged. The transformer is placed at the same location and in the same orientation throughout the experiment for repeatability of results. Heat removal is via natural convection plus radiation. The ambient temperature of the laboratory is confirmed to be within ± 2°C. All the temperature sensors are initially calibrated and their calibration is frequently checked throughout the experiment. The data logged into the computer is analyzed to derive the parameters of thermal model of Fig. 7.

The measured resistance of primary and secondary windings in the cold state is 0.2186 Ω and 0.0075 Ω, respectively.

The rated maximum primary and secondary rms current of prototype transformers are 5.6 A and 33.5 A respectively. Therefore, to measure the temperature rise of primary winding due to losses in itself, a dc current (4, 5, 6 and 7 A) was passed through the primary winding in steps. Similarly, 20, 30, 40 and 50 A current was passed through the secondary winding. Measured temperature rise of primary and secondary winding under different test conditions was calculated. Results for the conventional planar transformer are shown in Fig. 9.

The procedure is repeated for the extended-core planar transformer to determine the temperature rise of windings under different test conditions. Figure 10 shows the temperature rise of primary winding due to losses in primary in conventional as well as extended-core planar transformer. The superior thermal performance of the proposed novel extended-core geometry is now evident. The temperature rise of the primary winding with the extended core geometry is reduced almost to the half as compared to the conventional planar transformer without core extensions.

The data obtained from the tests is used to derive the parameters of the thermal equivalent circuit (see Fig. 7). Table 2 summarizes various thermal resistances of the planar transformer in conventional and extended-core geometry. The lower values of thermal resistances in extended-core planar transformer are indicative of superior thermal performance.

The parameters of thermal model are obtained by creating dc losses in individual winding sections. During normal operation of the transformer the winding losses co-exist simultaneously. It is possible using the model to predict the average temperature of either winding under this condition. With reference to the model of Fig. 7, average temperature of each winding can be written as,

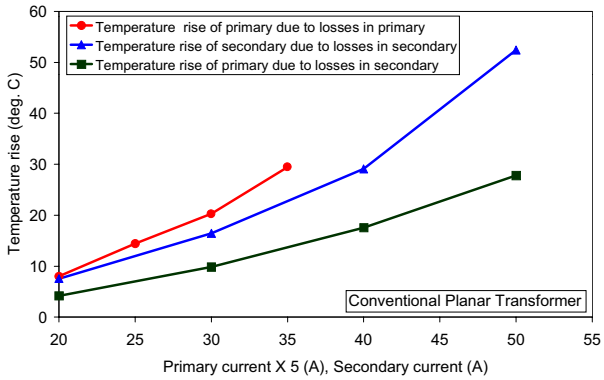

Fig.9: Experimentally measured temperature rise of windings of the conventional transformer under different test conditions.

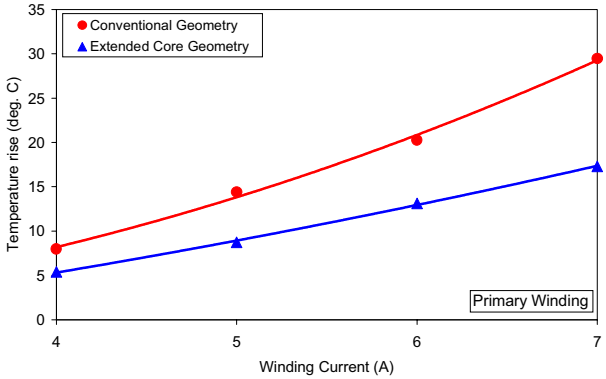

Fig.10: Comparison of thermal performance of conventional and extended-core geometry. Temperature rise of primary winding due to losses in the primary winding only. The results clearly show that the winding temperature rise in proposed extended-core geometry is smaller than that in the conventional transformer.

TABLE 2

VAULES OF VARIOUS THERMAL RESISTANCES IN PLANAR TRANSFORMER MODEL

Thermal resistance	Value ($^oC/W$)	
	Conventional	Extended-core
R_{ph}	2.91	1.05
R_{sh}	2.39	1.70
R_{ps}	2.18	0.89
R_{ha}	0.59	0.59

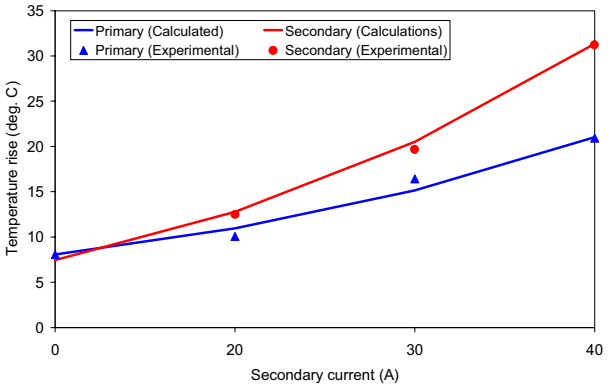

Fig.11: Experimental validation of model parameters for extended-core geometry. Continuous curve shows the calculated temperature rise of the windings and the solid markers show the experimental measurements when the primary current is 6 A and secondary current is increased in steps from 0 to 40 A.

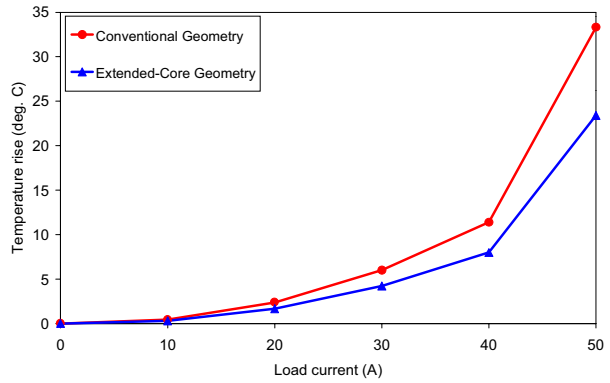

Fig.12: Application of the thermal model to predict the temperature rise of primary winding in conventional and extended-core transformers in operating conditions in forward converter as the load current varies from 0 to 50 A.

$$T_p - T_h = \frac{R_{ph}}{R_{ph} + R_{ps} + R_{sh}} \left(R_{sh} P_s + \left(R_{ps} + R_{sh} \right) P_p \right) \qquad (8)$$

$$T_s - T_h = \frac{R_{sh}}{R_{ph} + R_{ps} + R_{sh}} \left(R_{ph} P_p + \left(R_{ps} + R_{ph} \right) P_s \right) \qquad (9)$$

The accuracy of the model must be validated first, before applying the model for predictions. To validate the accuracy of derived model parameters, for instance, of extended-core prototype, 6 A dc was passed through primary winding and current of secondary winding was varied in steps from 0 to 40 A. In each step rise in the temperature of primary and secondary winding is noted and compared with the predicted values. Figure 11 shows that the experimental results and predicted values are in close agreement and thus validate the accuracy of the model.

The model can now be used to predict the winding temperature rise when it is used in a 1 kW (20V/50A) power supply. Figure 12 shows predicted temperature rise of the primary winding as a function of load current. The winding temperature rise with extended-core geometry is seen to be lower.

VI. SHIELDING EFFECT OF THE EXTENDED-CORE GEOMETRY

It is intuitive that the ferrite core placed over a winding carrying high frequency current shields the surroundings from the radiated field. The merit of proposed extended-core geometry in this respect is illustrated here with the help of finite-element analysis.

2-D magentostatic finite element analysis is also performed for winding section outside the core in conventional and proposed geometry. The results are shown in Fig. 13. It can be observed that the fringing flux is contained by the extended core thereby reducing radiated EMI. In this respect, it is expected that a U-U type core extension can be better than simple I-type core extension since the former covers the windings more completely.

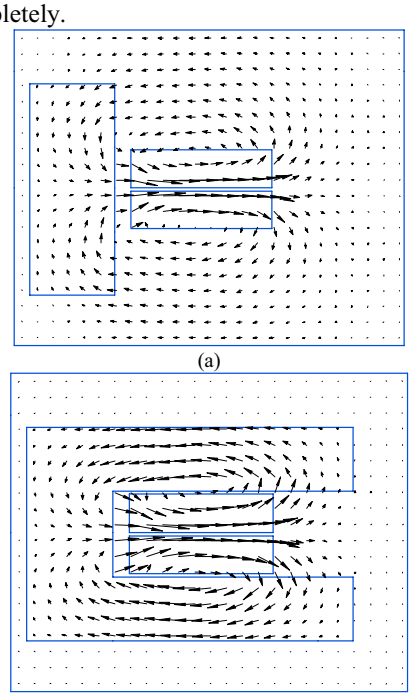

Fig.13: Results of 2-D finite element simulations for protruding winding sections planar transformer with (a) conventional structure, and, (b) I-type extended-core geometry.

VII. Cost and Manufacturability of Extended-Core Planar Transformer

The merits of the proposed extended-core planar transformer, namely, better thermal performance and effective shielding comes at the cost of core pieces (I-type or U-type). However, required core sections for the extension over the protruding winding sections are not of extraordinary profile. In case of I-type core extension, the standard I-type cores available from the ferrite manufacturer can be used directly. No additional machining, grinding and milling is required. Therefore the additional cost of implementing the proposed extended-core geometry is not significant. Similarly, U-type core extensions can be realized by standard U-type cores, if available from the manufacturer. Otherwise, the required U-section can be made by grinding the central limb of standard E-section. In this case, the additional process cost must be considered.

Since the extended-core geometry is a simple improvement over the conventional planar transformers resulting in significant performance improvement, the conventional manufacturing process is not greatly altered. Additional core pieces and clamps are the only extra components required.

VIII. Conclusions

The limitations of conventional planar transformer are identified. The protruding winding sections result in ineffective heat transfer from windings and give rise to radiated EMI. A simple solution to these problems is proposed in this paper. The proposed extended-core geometry is shown to enhance the heat removal from the windings and also shield the uncovered winding sections to reduce stray fields. The thermal model is defined and a systematic experimental procedure to derive model parameters is described. It is shown that with simple laboratory experiments the thermal behaviour of the structure can be investigated. The model can be applied to predict temperature of windings under different operating conditions in its intended application. Preliminary results of finite-element analysis confirm the shielding effect of the extended-core geometry. More importantly, complex profile and manufacturing process is not required to make additional core pieces. Standard available cores can be readily used. Therefore, the additional cost of implementation of extended-core planar transformer is negligible.

It is important to note that the accuracy and applicability of proposed experimental method for thermal characterization is limited only for planar structures. In non-planar structures the distances of core center point and the windings from the surfaces are large. This causes large temperature gradients and creates hot-spots. The average temperature measurement is thus erroneous.

Acknowledgement

The authors acknowledge the assistance of Mr. Vinod Somkuwar, Mr. T. S. Rawat and Mr. M. K. Koli during the fabrication and testing of the prototypes.

References

[1] "Design of planar power transformers" *Philips Magnetic Products,* Application note.

[2] D. Linde, C. Boon, J. Klassens, "Design of high frequency planar transformer in multilayer technology", *IEEE Trans. Ind. Electron*, vol. 38, no. 2, April 1991.

[3] Wai-Keung Mo, "Design and analysis of high frequency low-profile magnetics*", Ph. D. Thesis*, The Hong Kong Polytechnic University Department of Electronic and Informantion Engineering, June 1998.

[4] S. Ben Yaakov, "Planar magnetics benefits in HF power conversion", *Electronics for you,* January 1996.

[5] A. Lotfi, N. Dai, G. Skutt, W. Taibez, F. Lee, "A comparative study of high-frequency low-profile planar transformer technologies", *EPE*, 1993.